



Identifying Wind and Solar Ramping Events

Preprint

A. Florita, B.-M. Hodge, and K. Orwig

*To be presented at the IEEE Green Technologies Conference
Denver, Colorado
April 4–5, 2013*

NREL is a national laboratory of the U.S. Department of Energy, Office of Energy Efficiency & Renewable Energy, operated by the Alliance for Sustainable Energy, LLC.

Conference Paper
NREL/CP-5500-57447
January 2013

Contract No. DE-AC36-08GO28308

NOTICE

The submitted manuscript has been offered by an employee of the Alliance for Sustainable Energy, LLC (Alliance), a contractor of the US Government under Contract No. DE-AC36-08GO28308. Accordingly, the US Government and Alliance retain a nonexclusive royalty-free license to publish or reproduce the published form of this contribution, or allow others to do so, for US Government purposes.

This report was prepared as an account of work sponsored by an agency of the United States government. Neither the United States government nor any agency thereof, nor any of their employees, makes any warranty, express or implied, or assumes any legal liability or responsibility for the accuracy, completeness, or usefulness of any information, apparatus, product, or process disclosed, or represents that its use would not infringe privately owned rights. Reference herein to any specific commercial product, process, or service by trade name, trademark, manufacturer, or otherwise does not necessarily constitute or imply its endorsement, recommendation, or favoring by the United States government or any agency thereof. The views and opinions of authors expressed herein do not necessarily state or reflect those of the United States government or any agency thereof.

Available electronically at <http://www.osti.gov/bridge>

Available for a processing fee to U.S. Department of Energy and its contractors, in paper, from:

U.S. Department of Energy
Office of Scientific and Technical Information
P.O. Box 62
Oak Ridge, TN 37831-0062
phone: 865.576.8401
fax: 865.576.5728
email: <mailto:reports@adonis.osti.gov>

Available for sale to the public, in paper, from:

U.S. Department of Commerce
National Technical Information Service
5285 Port Royal Road
Springfield, VA 22161
phone: 800.553.6847
fax: 703.605.6900
email: orders@ntis.fedworld.gov
online ordering: <http://www.ntis.gov/help/ordermethods.aspx>

Cover Photos: (left to right) PIX 16416, PIX 17423, PIX 16560, PIX 17613, PIX 17436, PIX 17721



Printed on paper containing at least 50% wastepaper, including 10% post consumer waste.

Identifying Wind and Solar Ramping Events

Anthony Florita, Bri-Mathias Hodge, and Kirsten Orwig
Transmission and Grid Integration Group
National Renewable Energy Laboratory
Golden, CO USA

Abstract—Wind and solar power are playing an increasing role in the electrical grid, but their inherent power variability can augment uncertainties in the operation of power systems. One solution to help mitigate the impacts and provide more flexibility is enhanced wind and solar power forecasting; however, its relative utility is also uncertain. Within the variability of solar and wind power, repercussions from large ramping events are of primary concern. At the same time, there is no clear definition of what constitutes a ramping event, with various criteria used in different operational areas. Here, the swinging door algorithm, originally used for data compression in trend logging, is applied to identify variable generation ramping events from historic operational data. The identification of ramps in a simple and automated fashion is a critical task that feeds into a larger work of 1) defining novel metrics for wind and solar power forecasting that attempt to capture the true impact of forecast errors on system operations and economics, and 2) informing various power system models in a data-driven manner for superior exploratory simulation research. Both allow inference on sensitivities and meaningful correlations, as well as quantify the value of probabilistic approaches for future use in practice.

Index Terms—wind energy, solar energy, forecasting, time series analysis

I. INTRODUCTION

The increasing amounts of wind and solar power capacity being installed in the electrical system are causing more concern from system operators about the variable and uncertain nature of these generators. To an extent, power system operations are already able to handle variability and uncertainty, e.g., power demand. Existing techniques include regulation reserves, load-following reserves, and sub-hourly economic dispatch. However, in simplistic terms, the uncertainty in load, now coupled with increasing levels of uncertainty in generation, can lead to wider distributions of uncertainty for all variables and parameters of interest; responding to variability under increased uncertainty is all the more difficult. Enhanced wind and solar power forecasting can help address some of these concerns through the reduction of uncertainty faced by the system of interest. Because there are mechanisms in place to handle small amounts of uncertainty and variability, power system operators place primary emphasis on better understanding the impact of extreme events (e.g., large ramps), which can have significant influence on system economics and reliability. Secondary concern is for uniform power forecasting improvements for enhanced planning applications.

Wind and solar ramps can occur at different timescales, geographic scales, and in both the positive and negative directions. Variable generation forecasting can help remove some of the uncertainty involved with the power supply, but may have trouble forecasting large ramping events. The numerical weather prediction models often used for forecasting are generally good at predicting roughly when a ramping event may occur; however, there are two main ways in which inaccurate forecasting of ramp events can lead to large errors: ramp magnitude and timing errors. In ramp magnitude errors, a ramp is forecast, but the actual value changes significantly more/less than was forecast. In ramp timing errors, the actual ramp in power significantly leads/lags the forecast time. Of course, both errors can occur simultaneously, which indicates a poor forecast. It is the hope that offline ramp analyses, coupled with extensive unit commitment and dispatch simulation studies, will allow the synthesis of knowledge for enhanced dispatch in cases of large variable generation power ramps.

The automated identification of ramping events must be computationally inexpensive to justify online applications, but can also help facilitate the improvement of forecasting algorithms by providing metrics on how well ramping events are captured. Kamath analyzed wind ramping events in the Bonneville Power Administration area using two definitions of ramping [1]. The first definition was simply the slope of change between two points; the second considered the minimum and maximum values of generation between two points. Zheng and Kusiak [2] focused on forecasting wind power ramping events. They employed the rate of change of wind plant power over a 10-minute interval to define ramps. Hodge et al. [3] used similar fixed-point definitions to identify and characterize the number of ramping events that occurred for solar power at different timescales. Hansen et al. [4] used the swinging door algorithm to characterize irradiance time series data in the Southwest United States. Because of the flexibility and simplicity of the algorithm, both wind and solar power ramps over varying time frames can be identified.

II. SWINGING DOOR ALGORITHM

In this work, we propose the application of an algorithm from the area of data compression, known as the swinging door algorithm [5], to identify wind and solar power ramping events. Its computational and structural simplicity, requiring only one parameter in its definition, are favorable attributes considering its robustness in the face of noisy data.

Ramps are typically extracted through a linear piecewise approximation to the original time series of data. If extracting ramps from measured data, the approximation can be thought of as a disregard for the noise inherent to the measurement process and/or insignificant changes. If extracting ramps from simulated data, the approximation can be thought of solely as disregard for the insignificant changes. In either case, the focus of ramp extraction is placed on the significant linear ramps (in terms of magnitude and duration) present in the dataset.

Mathematically speaking, a ramp is quantified by its instantaneous rate of change, its derivative, $\frac{dG}{dt}$, and is approximated initially by a local ratio of differences: $\frac{dG}{dt} = \frac{G(k)-G(k-1)}{k-(k-1)}$. The discrete-time nature of either the measured or simulated data easily allows such a calculation. However, the point of ramp extraction is to determine a trend in a sequence of local derivatives and the magnitude and duration of such a trend. For example, when considering a time series of power, the local derivative (ramp) from the first two points may be $\frac{3.0}{2-1} = 3 \text{ MW}$ and from the second and third points $\frac{3.2}{3-2} = 3.2 \text{ MW}$. The trend is apparent and the average ramp is 3.1 MW over the three discrete-time samples. The question of interest is when a particular ramp has started and/or when the local derivative has changed to the point it can no longer be considered part of a particular ramp.

Figure 1 illustrates a simplified example of a signal and the ramps that may be extracted. Of course, a realistic time series of wind or solar power is much more complicated, but the same strategies and goals for the extraction of ramps apply as described here. The measurement points are discrete-time samples, and the spline fit is included in the figure to show what the continuous process may resemble. The identified ramps are nearly of equal magnitude, but in general this will not be the case. It is somewhat easy to visually discern the ramps (trends) even though it is apparent the sign of the slope can change within a particular ramp. Although noise is inherent to any real measured data, here there are no assumptions about the probability density of a realization and the piecewise linear approximation to the time series is anchored to dominant points. Considering a threshold for the ramp trend and anchoring the piecewise linear approximation to measurement points allows for reduced sensitivity to inflection points and other insignificant fluctuations.

The swinging door algorithm allows the extraction of ramps in a signal, in a piecewise linear fashion, while allowing for consideration of a threshold parameter influencing its sensitivity to ramp variations. The only tunable parameter is ϵ , the width of one “door” in the algorithm (as shown in Figure 2) that directly allows the (threshold) sensitivity to noise and/or insignificant fluctuations to be specified. If the tolerance is very low (a small ϵ value), the ramp extraction algorithm will identify many small ramps as it basically traces the original signal, violates the threshold, and starts over. If the tolerance is very high (a large ϵ value), the algorithm will identify a few large ramps as it is under constrained and a large fluctuation is required for the threshold to be violated. In the figure, it should

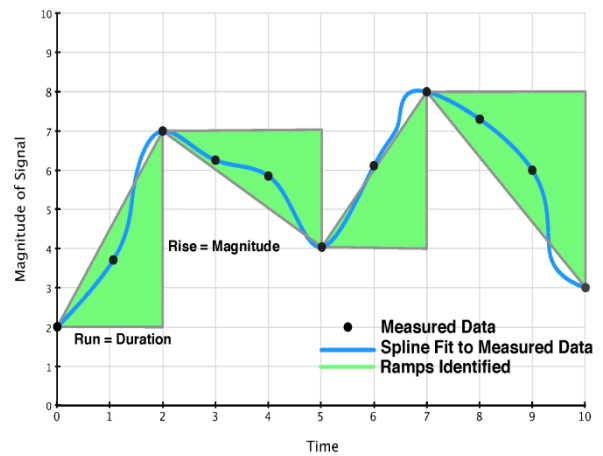


Figure 1. Example of the piecewise linear approximation to a time series for ramp extraction and analysis; the scale is arbitrary for explanation purposes.

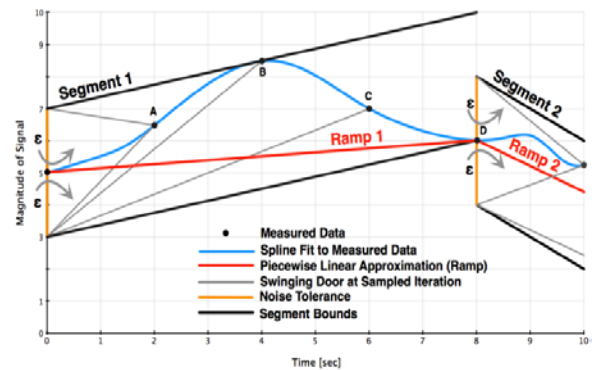


Figure 2. The swinging door algorithm for the extraction of ramps in power from the time series; the scale is arbitrary for explanation purposes.

be noted the scale is arbitrary for the purposes of explanation, and in general the signal magnitude is much larger than the scale of the threshold bounds.

From Figure 2, the swinging door algorithm is briefly described: 1) the initial (dominant) point, or new (ramp segment) iteration of the algorithm, is on the y-axis and threshold doors of width ϵ are placed above and below it; 2) a new point A is acquired and the doors “swing open,” as indicated, to include the point – i.e., lines are drawn from the doors’ hinges to the point; 3) a new point B is acquired and lines are again drawn (updated) to intersect at B; 4) a new point C is acquired, but there has been an inflection in the signal, and the swinging doors open only to accommodate new points in a ramp segment iteration, so the top door (extended line) remains in its angle position above C and the lower door line is drawn to point C – further extension of the lines would result in an intersection at some point in the future; 5) a new point D is acquired; again the top door (line) angle position is not updated, and the lower door line is drawn to point D. The lines

are now parallel (or do not intersect in the future), which starts a new iteration of the algorithm – i.e. the threshold has been exceeded when the line angle from the hinges to their most open position is greater than or equal to parallel. The threshold could be violated somewhere between C and D, but because of the discrete-time nature of the approximation, a new iteration would still start at D. The piecewise linear approximation (the ramp, shown in red) starts at the end of the previous iteration (dominant point) and ends when the threshold is exceeded (next dominant point).

Ramp sign changes are an indicator of fluctuation, but it is not obvious what an insignificant fluctuation is when considering noisy measured data and/or actual (but slight) power variations. There are two applications that are noted for defining the threshold and thus what is considered an insignificant fluctuation: 1) according to the accuracy of the measurement device as defined by its distribution of measurement uncertainty, or 2) according to the utility of the measure as defined by power system economics and its relative importance in driving operations. In this work, neither application is explicitly employed, but the ϵ value varied to explore the sensitivity of ramp events extracted according to its value. Specifically, the ϵ value is set to a percentage of the maximum capacity observed in the time frame of interest.

Figure 3 shows a typical example in the extraction of ramps from a large wind farm over a two-day period. The power profile, composed of hourly data, is variable but somewhat smooth because of the diversity in power from individual turbines aggregating to cancel high-frequency variability, combined with time-averaged power output over the hour. Therefore, a rather high tolerance, ϵ value of 10% of maximum capacity, was used and provided an accurate piecewise linear approximation to the wind power profile.

Figures 4 and 5 show typical examples in the extraction of ramps from a solar plant over a two-day period, both using data sampled on a one-minute basis; first, the clear day of Figure 4, followed by the somewhat cloudy day of Figure 5. The power

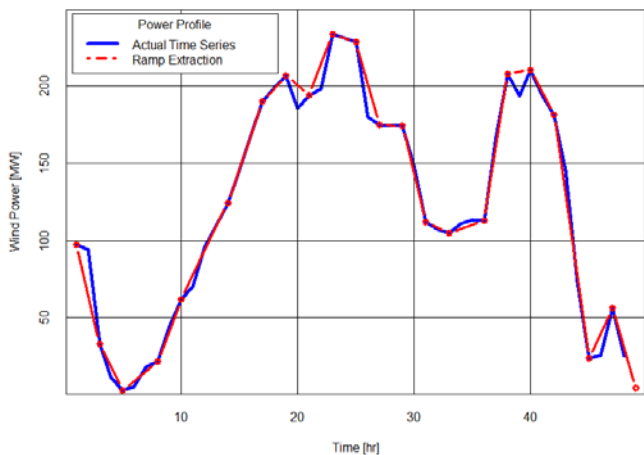


Figure 3. Typical example of ramp extraction from two days of power at a large wind farm, showing up and down ramps of large, medium, and insignificant nature.

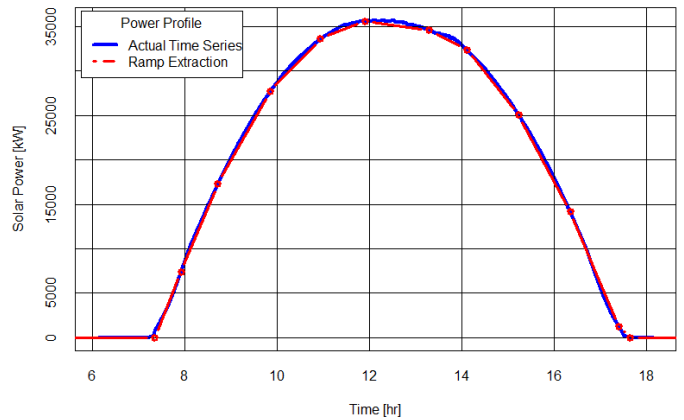


Figure 4. Typical example of ramp extraction from the first of two days of power at a PV solar plant, showing a clear day leading to a smooth profile.

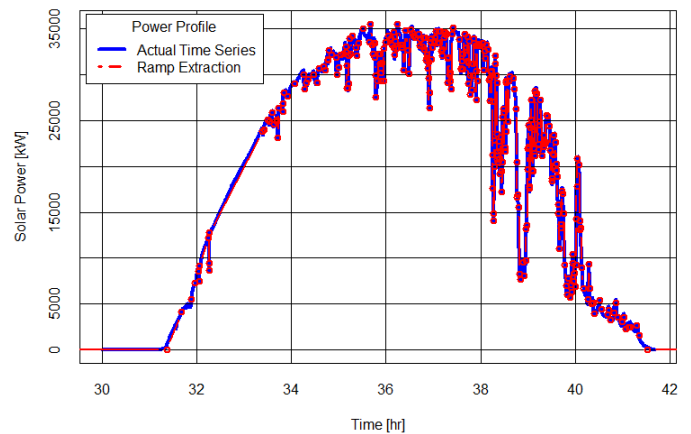


Figure 5. Typical example of ramp extraction from the second of two days of power at a PV solar plant, showing up and down ramps because of clouds.

profile is smooth in Figure 4 and shows high-frequency variability in Figure 5. A rather low tolerance, ϵ value of 1% of maximum capacity, was used and provided an accurate piecewise linear approximation to the solar power profile. However, it is apparent the ϵ choice introduces tradeoffs between the count of ramps and their approximation accuracy. That is, a clear day may be adequately described by fewer piecewise segments, whereas a cloudy day may require more for an adequate description. Economics of the system under consideration will likely determine the choice of ϵ .

III. WIND AND SOLAR DATA

To showcase the use of the swinging door algorithm for wind and solar power ramp detection, it was applied to various datasets. Wind data came from a wind plant in the Xcel Colorado territory with an approximate capacity of 300 MW; the discrete-time sample was 1 minute. The solar data came from Oahu and Maui, Hawaii, in association with the Hawaiian Solar Integration Study; the discrete-time sample was 1-second.

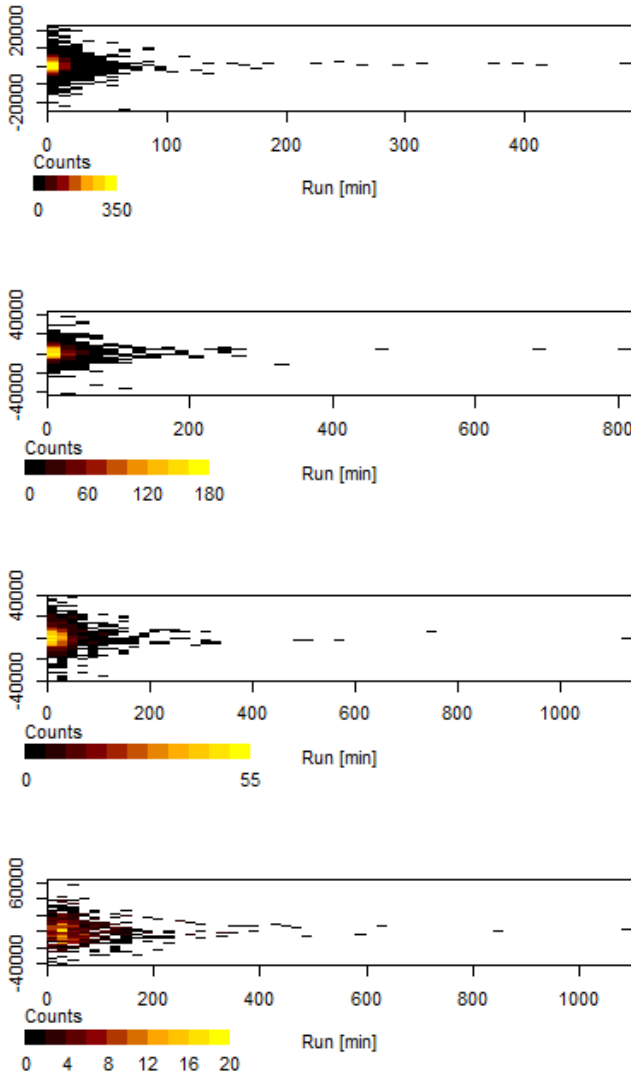


Figure 6. Bivariate distribution of wind power, ramp rise versus run, as a function of the ϵ value; top subplot is $\epsilon = 1\%$ maximum capacity in December, followed by $\epsilon = 2, 3,$ and 5% , respectively.

IV. RESULTS

The resolution of the extracted ramp events is a function of ϵ , which is informed by application specifics. The utility of a given magnitude of ramp event (as part of power system economics) was not considered here, but it is the subject of ongoing research toward understanding the probabilistic relationships of various systems. Typical wind and solar power examples were provided in this section, but the time resolution, geographic diversity, and extent of smoothing from plant aggregation were limited to the data available.

Ramp extractions were visualized by rise-run distributions. Figures 6 and 7 give the bivariate distributions of wind and solar power, respectively, as a function of various ϵ values; in both figures, the ϵ value was, from top-to-bottom subplots,

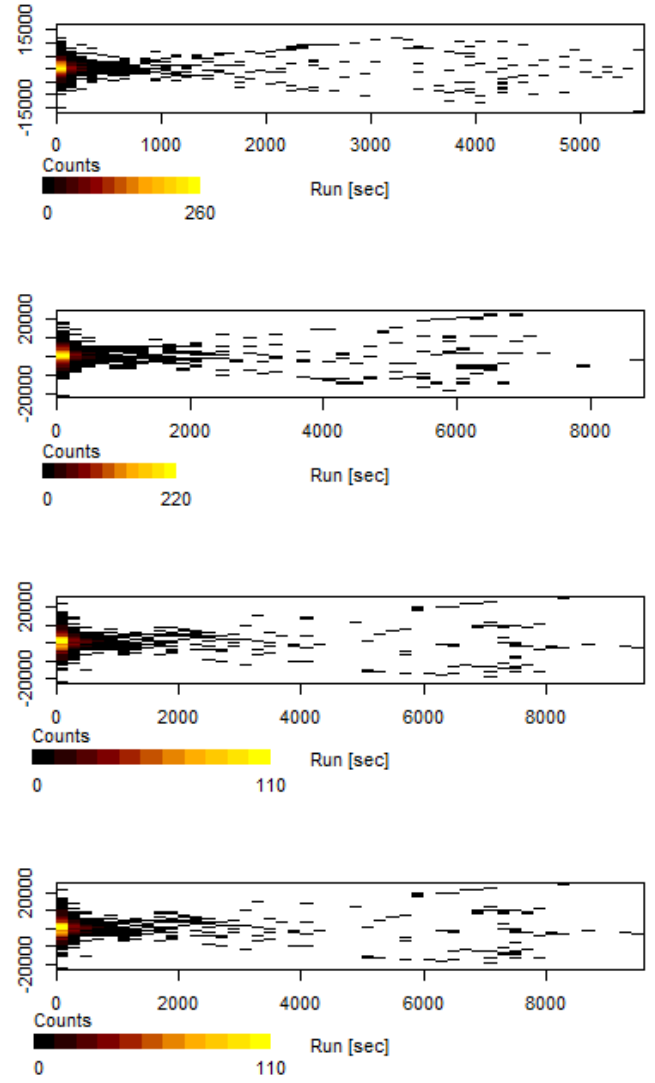


Figure 7. Bivariate distribution of solar power, ramp rise versus run, as a function of the ϵ value; top subplot is $\epsilon = 1\%$ maximum capacity in December, followed by $\epsilon = 2, 3,$ and 5% , respectively.

equal to 1, 2, 3, and 5% of the maximum capacity observed in the month of December.

From the wind power ramp extraction of Figure 6 (i.e., rise [MW] versus run [min]), it is noted that with lower tolerance, more ramps of longer duration were extracted. This would be expected, but it is also interesting to note how the distribution spreads within the more immediate (quick) ramp region. In the solar power ramp extraction of Figure 7 (rise [kW] versus run [s]), the same trends as the wind example were noted; however, there appeared to be a correlated “what goes up, must come down” pattern to the ramps because of the diurnal nature of solar irradiance. That is, there was an approximate balance of up and down ramps of similar magnitude and duration. Furthermore, the dispersion of ramps was driven by the plant (area) size and the December cloud cover.

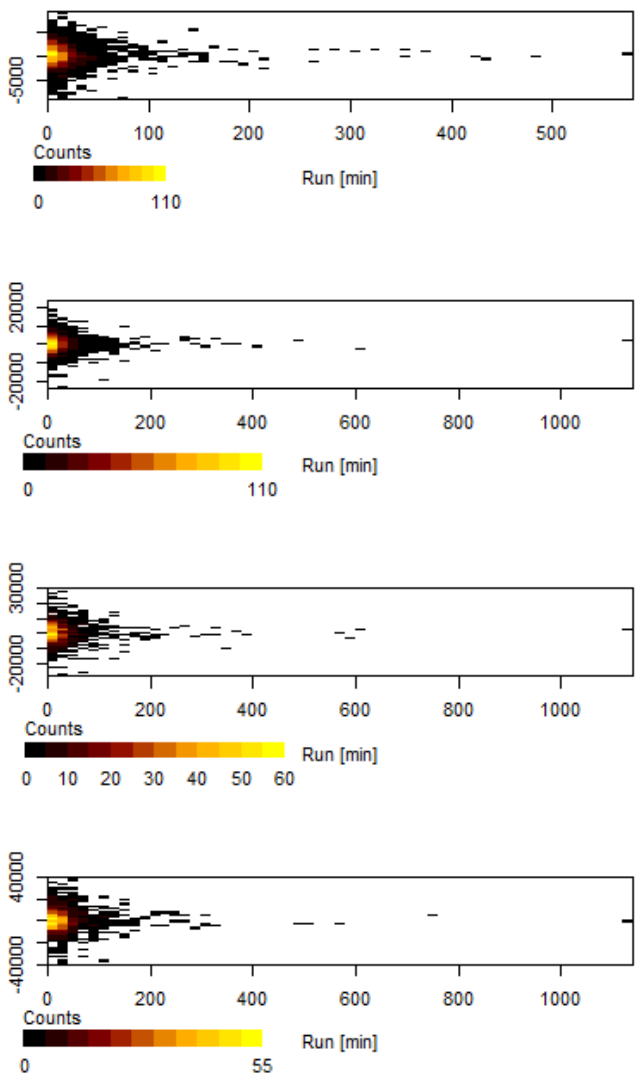


Figure 8. Bivariate distribution of wind power, ramp rise versus run, as a function of the aggregation level of wind turbines; top subplot is $\epsilon = 25\%$ total wind farm, followed by $\epsilon = 50, 75,$ and 100% , respectively. An $\epsilon = 3\%$ of the maximum capacity was used for the month of December.

As might be expected, smoothing from aggregation was observed in both power datasets and varied according to the size (area) of the total plant. In wind power, the downstream turbines generally experienced slower and more turbulent wind, and spatial correlations in power variability diminished with distance. In solar power, cloud cover seemed to have only influenced a portion of the array, and spatial correlations in power variability diminished with distance. In either case, and as is frequently observed, variability was smoothed with increasing plant (area) size.

It was of interest to determine the extent of smoothing observed in the extracted ramp events. Figures 8 and 9 give the bivariate distributions of wind and solar power, respectively, as

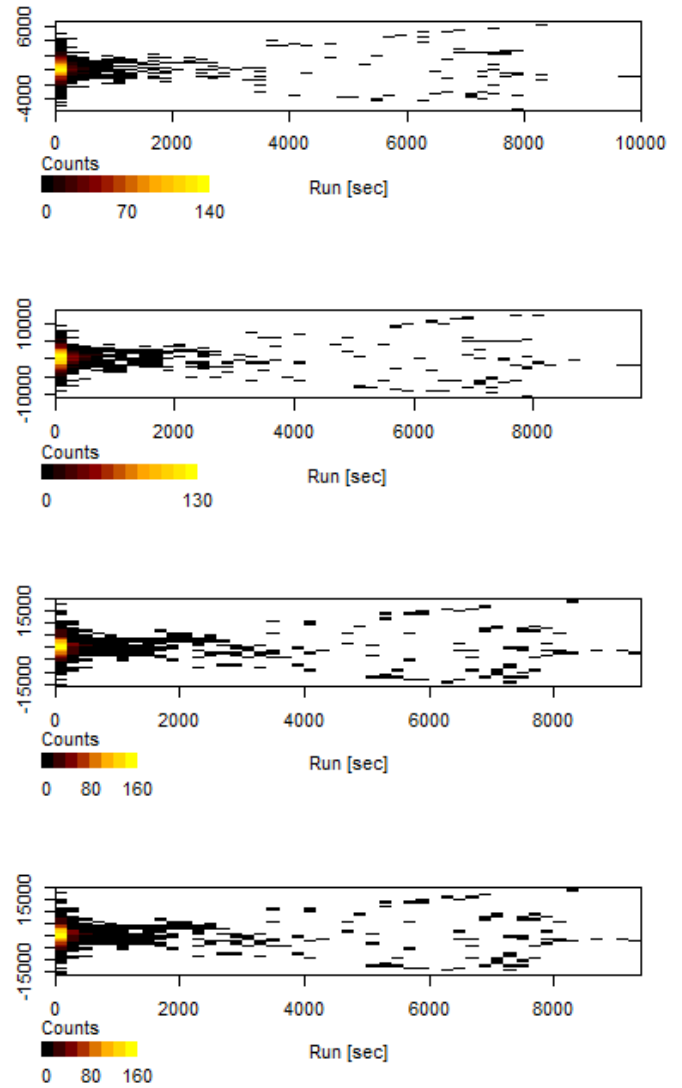


Figure 9. Bivariate distribution of solar power, ramp rise versus run, as a function of the aggregation level of PV modules; top subplot is $\epsilon = 25\%$ total plant, followed by $\epsilon = 50, 75,$ and 100% , respectively. An $\epsilon = 3\%$ of the maximum capacity was used for the month of December.

a function of levels of aggregation in either percentage of wind turbines or PV modules; in both figures, the percentage was, from top-to-bottom subplots, equal to 25, 50, 75, and 100% of the total fleet in the month of December. As shown by the wind power ramp extraction of Figure 8 (i.e. rise [MW] versus run [min]), there was a slight reduction in the dispersion of ramps as the aggregation level increased. In the solar power ramp extraction of Figure 9 (rise [kW] versus run [s]), the same trends as the wind example were noted; however, the correlated nature caused by diurnal behavior became more pronounced with increasing levels of aggregation. In addition, the frequency of more immediate (quick) ramps seemed to level off around one-half the total capacity of the PV solar plant.

V. CONCLUSIONS

The forecasting of solar and wind power ramps is a major area of concern in the field of variable generation forecasting. In this work, the application of a data compression technique to the identification of solar and wind power ramps was shown. Because these ramping events are one of the most pressing concerns of system operators in balancing areas with large penetrations of variable generation, this automated identification process is helpful toward creating algorithms and assessment metrics that can better forecast variable generation ramps and their economic impact.

One of the critical issues in wind and solar power forecasting is that the metrics used to assess forecasting techniques are simple statistical measures that do not take into account the factors that are most critical for power system operations. For example, because power systems have means by which they can compensate for small forecast errors, and large forecasting errors are both expensive and can present reliability concerns, it would be better to improve the forecasting for these extreme events, even at the cost of slightly decreased performance during the rest of the times. This is something that is very difficult to capture with the currently used statistical techniques in which the impact of a large number of small error events can overwhelm the impact of a small number of large error events.

Because ramping events comprise a large percentage of these large error events, their automated identification is an important step toward developing metrics that can be used to tune forecasting algorithms to consider their importance. In addition, similar identification techniques could be used actively in system operations. One possible example of how this could be used to improve operations would be an increase in reserves being triggered by the signal when a down ramp in power output had begun. The automated identification would also be useful in assessing probabilistic forecasts. Some system operators currently request that downward ramps in wind

power are forecast in a probabilistic manner, in a separate forecast product from the normal forecasts. These forecasts indicate degree-of-belief, giving the likelihood of a down ramp occurring in the specified time frame, and the automated identification techniques advocated here could lead to improvements in assessing system performance.

ACKNOWLEDGMENT

This work was supported by the U.S. Department of Energy under Contract No. DE-AC36-08-GO28308 with the National Renewable Energy Laboratory.

The authors would also like to thank Keith Parks at Xcel for the wind power data.

REFERENCES

- [1] C. Kamath, "Understanding wind ramp events through analysis of historical data," in *2010 IEEE PES Transmission and Distribution Conf. and Expo.*, New Orleans, LA, 2010.
- [2] H. Zheng and A. Kusiak, "Prediction of wind farm power ramp rates: A data-mining approach," *J. of Solar Energy Eng.*, vol. 131, 2009.
- [3] B.-M. Hodge, M. Hummon, and K. Orwig, "Solar ramping distributions over multiple timescales and weather patterns," in *The 1st Int. Workshop on Integration of Solar Power Into Power Systems*, Aarhus, Denmark, 2011.
- [4] C. Hansen, J. Stein, and A. Ellis, "Statistical criteria for characterizing irradiance time series," Sandia National Laboratories, Albuquerque, NM, 2010.
- [5] E. Bristol, "Swinging door trending: Adaptive trend recording?," in *International Standards for Automation*, 1990.